Optimized Load Shedding Approach for Grid-Connected DC Microgrid Systems under Realistic Constraints

Leonardo Trigueiro dos Santos, Manuela Sechilariu, Fabrice Locment

buildings

MDPI

Article

Optimized Load Shedding Approach for Grid-Connected DC Microgrid Systems under Realistic Constraints

Leonardo Trigueiro dos Santos, Manuela Sechilariu and Fabrice Locment *

Sorbonne University, Université de Technologie de Compiègne, Avenues EA 7284, Compiègne 60203, France; leonardo.trigueiro-dos-santos@utc.fr (L.T.d.S.); manuela.sechilariu@utc.fr (M.S.)

* Correspondence: fabrice.locment@utc.fr; Tel.:+33-3-44-23-73-17

Academic Editors: Gianpiero Evola and David Arditi

Received: 28 July 2016; Accepted: 5 December 2016; Published: 9 December 2016

Abstract: The microgrid system is an answer to the necessity of increasing renewable energy penetration and also works as a bridge for the future smart grid. Considering the microgrid system applied to commercial building equipped with photovoltaic sources, the usage of a DC microgrid architecture can improve the efficiency of the system, while ensuring robustness and reducing the overall energy cost. Given the power grid stress and the intermittency of the DC microgrid power production, backup power provision and load shedding operations may occur to stabilize the DC bus voltage. Based on the knapsack problem formulation, this paper presents a realistic optimization approach to shedding a building's appliances, considering the priority of each appliance, and also considering a minimum amount of load that must be attended. The problem is solved by mixed integer linear programming and the CPLEX solver. The proposed architecture ensures critical load supply and voltage stabilization through the real-time operation of the operational algorithm allowing the load shedding optimization approach to be applied without compromising the robustness of the system. The results obtained by simulation prove that the DC microgrid is able to supply the building power network by applying the load shedding optimization program to overcome, mainly, the renewable energy intermittency.

Keywords: DC microgrid; optimization; load shedding; knapsack problem; voltage stabilization

1. Introduction

In recent years, the appeal for the application of renewable energy sources has increased, given the awareness on environmental issues, such as climate change and greenhouse gas emission. This pressure for clean and environmentally-friendly energy, along with the liberalized electric market, and the demand of efficient, reliable, and diversified energy sources, have led to an increasing interest in renewable power generation [1]. The microgrid approach was designed as a bridge technology towards the smart grid system that intends to increase small-scale energy generation and minimize the energy cost [2].

The low power generation capacity on distributed sources has motivated the integration of distributed generation units aiming to increase power generator capacity, but since most distributed generation units, especially renewable distributed generation units, produce an intermittent power, the application of distributed generation units without a distributed storage system severely curtails the renewable energy penetration [3]. Given this limitation, power electronics devices have become a key point in microgrid development [4].

To overcome this limitation, and aiming to develop a bridge technology towards the future smart grid, the microgrid grid concept was proposed. The microgrid systems can be classified in

three different groups given its architecture. AC microgrid systems adopt the voltage and frequency standards applied in most conventional distribution systems [4]; the DC microgrid, idealized to be used in environments where DC loads are becoming predominant; and a hybrid microgrid working with two different buses, one AC and one DC. This paper is concerned about DC microgrid architectures. The operation of a DC microgrid is similar to the AC microgrid system and the continuous approach is mainly adopted to use the DC energy generated by the renewable distributed generation units in its natural form. By adopting the DC microgrid solution, part of the conversions necessary in the AC architecture can be avoided increasing the overall efficiency of the system. Nevertheless, in the DC architecture, a conversion is necessary at the point of common coupling (PCC) to be able to exchange power with the main grid [5]. Since photovoltaic (PV) panels have grown as one of the most commonly used renewable sources in urban areas, and DC loads could become predominant in commercial buildings [6], the DC microgrid architecture is proposed and studied in a grid-connected configuration using PV energy as the renewable source and an electrochemical storage system. The control strategies may comprehend just the local control, based on local measures, a power management strategy, included in centralized and decentralized approaches, or more layers, such as in the present work where an optimization layer is implemented.

The challenges faced to implement the microgrid concept, regardless of the type of microgrid, are depicted in [7], where the fact that the integration of distributed generators/loads and interaction between all nodes within a microgrid substantially increases the complexity of control techniques, communication, and power system technology is highlighted, reflecting on many questions about power quality, protection, stability, reliability, and efficiency. In addition to the already presented general challenges, and considering the intended use of the microgrid concept in commercial building applications, some new challenges are presented in [8]. The management and engineering operations of these buildings typically include end-user operations, heating ventilation and air conditioning, etc. This system is designed to perform the control of those units independently from each other, therefore, the absence of an integrated unit is presented in [8] as one of the major issues to the application of the microgrid concept in commercial buildings.

The power exchanged with the main grid and the storage system are mainly responsible for ensuring the power balance of the system, while coping with the intermittency problems tied with the renewable sources. However, once the operational constraints imposed to the power exchanged with the main grid and the storage system usage are reached, it is necessary to perform a load shedding to ensure the power balance and, therefore, voltage stability.

Load shedding is commonly defined as the amount of load that must be instantly shed, considering operational conditions and priorities. Some of the approaches are based on game theory methods and consider loads with a continuous range of values, ignoring the discrete characteristic of the load power demand [9–13]. In [9] a load control strategy named Distributed Interruptible Load Shedding is presented to share the load shedding necessity among the greatest possible group of users, to minimize the impact to each individual user. The disadvantage of this method is performing a probabilistic characterization of the load based on a Gaussian distribution of what is a possible limitation to certain cases where this distribution does not fit the desired profile, as pointed out by the authors. In [10], the authors focused on the necessity of performing load shedding in a distributed generation utility, during islanding operation mode, to ensure power balance. A combination of adaptive under-frequency load shedding and state estimation is proposed to solve this problem. In [11], aiming to replace the conventional load shedding methods, an intelligent approach is proposed. The conventional methods such as: breaker interlock scheme, under-frequency relay and programmable logic controllers described in [11] are slow and with low accuracy when calculating the amount of load to be shed. The load shedding method proposed in [11] is based on a computerized power management technology and aims to: recognize different patterns in order to predict the system response; make reliable decisions; and identify the minimum amount of load necessary to maintain system stability. The disadvantages of this method are the requirements to be met to design and

tune, such as a knowledge base obtained from offline system simulations, system dependencies, and continually-updated dynamic load shed tables. In [12], a load shedding approach is proposed for DC microgrid systems; the lack of communication to perform the load shedding is presented as the main advantage of the proposed method. Nevertheless, it becomes impossible to optimize the load shedding behavior, because in this method the appliances are ranked from the lowest to the highest to be shed in order, given the DC voltage fluctuation. In [13], the concept of a power buffer is introduced, stretching the time scale of the transient dynamic, diminishing the impact of tight converter regulation, and the load shedding is studied in depth to be used as an asset in a DC smart grid structure. Different control strategies are proposed: given the nature of the load, e.g., a resistive load, such as incandescent light, it does not necessarily need to be turned off completely but, instead, the amount of power sent to those sources could be reduced. The control strategy is also influenced by the aforementioned power buffer. If the voltage drops for a long time, the power buffer will not be able to reject this fluctuation and a different action, such as load shedding, is necessary to ensure voltage stability. This paper validates the usage of the load as an asset to perform energy management in DC smart grid systems but has not addressed itself to the optimum load shedding/restoration problem.

This paper aims to improve the DC microgrid approach introduced in [14,15] by introducing a demand-side management strategy, based on a more realistic load shedding/restoration algorithm. In [14] the main goal was to present the concept of an optimized approach to solve the energy management problem in a microgrid environment using a simple load profile with a continuous approach to the load shedding problem. The main focus was to present the supervision structure while the problem of the load shedding and restoration were not addressed. In [15] the model and concept presented in [14] were validated in the experimental platform, corroborating the conclusions presented in [14] and the applicability of the proposed microgrid concept. In [16], the concept depicted in [14,15] was translated to the isolated DC microgrid case, where a micro turbine was assumed to have only two possible states, disconnected or at the rated power, but the problem of load shedding and restoration was not addressed.

Since the designed structure for the presented microgrid system has proven its value, we decided to go one step further, focusing on the load shedding algorithm, in a realistic load profile. Instead of the continuous approach discussed before and presented in [14–16] as well, the proposed load shedding approach needs to respect the power, priority, and the discrete dynamic of each connected appliance. Other key aspects of the load shedding algorithm are the optimized load shedding, smart restoration, and a critical load level constraint to be respected ensuring that certain amounts of load shall not be shed under any circumstance.

Section 2 presents the grid-connected DC microgrid system, the supervision strategy, and the operational layer. Section 3 describes the load shedding/restoration approach and the knapsack optimization problem formulation. Section 4 describes the results obtained by simulation and gives analysis and discussion, and Section 5 presents the conclusions.

2. Grid-Connected DC Microgrid System

A typical grid-connected DC microgrid, aimed at building integration and increasing the overall efficiency of the system [1] is presented in Figure 1. Considering the environments where DC loads are becoming more and more common, e.g., commercial buildings and data centers, the DC microgrid approach becomes more interesting from the energetic efficiency point of view [16].

The proposed grid-connected DC microgrid consists of PV building-integrated sources, a storage system, and a main grid connection. The bidirectional connections with the main grid and the storage aim to supply the building's DC appliances, and sell or store the energy surplus.

Based on the microgrid power balance and considering that, ideally, the entire load should be supplied and all PV energy should be consumed, the two controllable power sources available to regulate the power balance of the system are the storage and the main grid, respecting the system presented in Figure 2. Knowing that the storage and main grid are capable of supplying, as well as

absorbing, energy from the microgrid, a storage priority strategy is adopted when the storage system is used to supply and to absorb energy from the system; thus, the main grid acts only as a backup source, being used only when the storage system is not capable of attending the system necessities by itself.

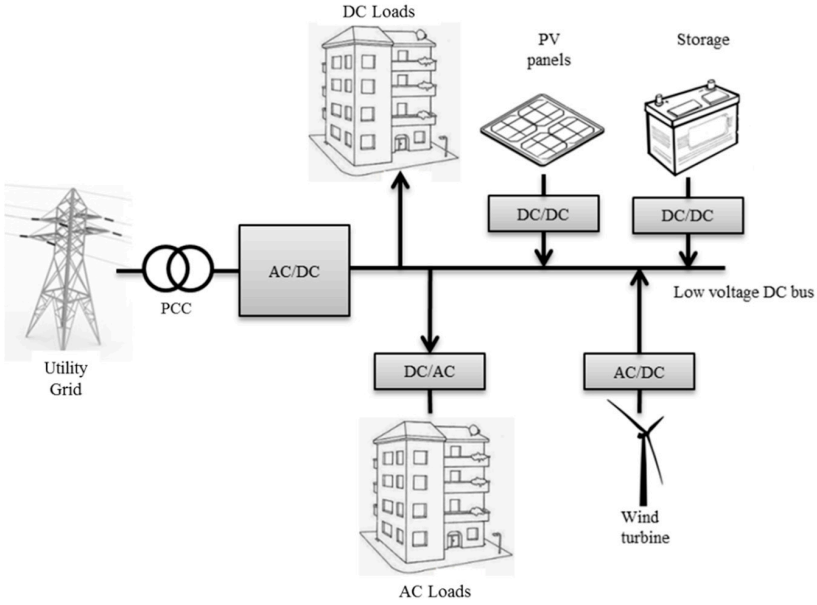

Figure 1. General DC microgrid architecture.

It is considered that the microgrid is able to ensure load supply while respecting the main grid limits imposed to the system through smart grid messages. The microgrid is assumed to have the necessary interface to exchange messages with the smart grid. The detailed microgrid power flow can be seen in Figure 2.

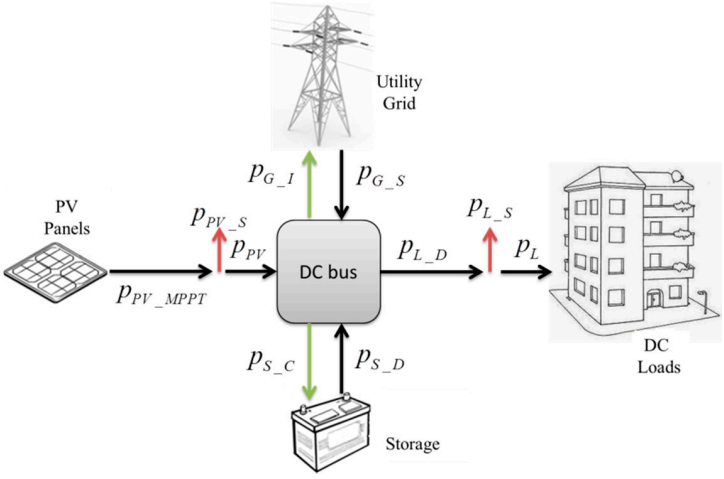

Figure 2. Proposed grid-connected DC microgrid power flow exchange.

The following powers are used: p_{G_I} is the power injected by the microgrid system into the main grid; p_{G_S} is the power bought from the main grid; p_{L_D} represents the total load power demand; p_{L_S} is the amount of load power shed; p_L is the load power demand supplied by the system; p_{S_D} is the power taken from the storage system, discharging it; p_{S_C} is the power injected into the storage system, charging it; p_{PV_MPPT} is the instant maximum power production from the PV system; p_{PV_S} is the PV power shed; and p_{PV} is the PV power consumed by the microgrid system.

2.1. Supervisory System

Aiming to interact with the smart grid environment as well as with the end-user, a supervisory system is proposed. The proposed supervisory system is a centralized approach where all of the available data about the microgrid system is concentrated in one main system, as presented in Figure 3. The power control, represented by the operational algorithm has, as its main goal, to keep the instantaneous power balance in the microgrid system respecting the main grid constraints as well as sources and load constraints. Figure 3 presents the interconnection between each implemented algorithm necessary to build the described supervisory framework.

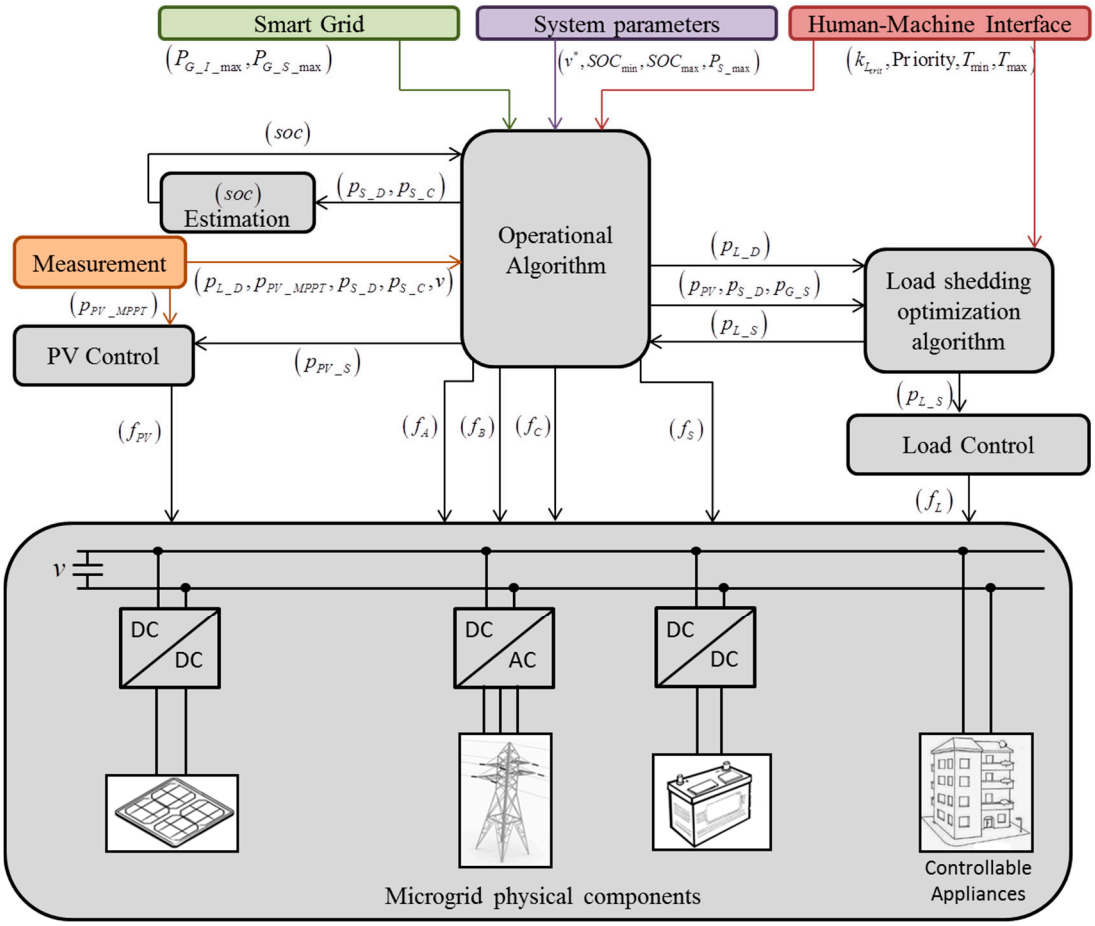

Figure 3. Supervisory and power control structure.

The structure presented in Figure 3 depicts how the information flows from different sources and how it interacts with the proposed algorithms. From the smart grid the information arrives regarding the maximum power allowed to be injected into the main grid, $P_{G\_I\_max}$, and the maximum allowed power to be used from the main grid to supply the microgrid system, $P_{G\_S\_max}$. These limits are supposed to be imposed by the distribution operator system through smart grid messages; they are translated as rigid constraints, meaning that the power exchanged with the main grid can never cross the imposed limits.

The smart grid block emulates the communication layer between the distribution system operator of the main grid and the microgrid system. It is assumed that this communication layer has the capability of sending information about the tariffing system and usage grid limitation to the microgrid as well as receiving back information about the grid usage prediction from the microgrid system.

The system parameters block represents the group of parameters related with the system conception and physical limitations, with v^* being the DC bus voltage reference, and $P_{S\_\max}$ being the maximum instant power allowed to be exchanged with the storage system in both senses.

The human-machine interface communicates with both the operational algorithm and the load shedding/restoration algorithm by sending information about the appliances' priorities and appliance shedding time limits $T_{\min}$,$T_{\max}$. as well as the information about the critical load level $k_{L_{crit}}$.

The state of charge (*soc*) estimation block, using the information about the power exchanged with the storage system p_{S_D},p_{S_C} estimates the actual *soc*. The energy exchanged with the storage system is limited by the maximum and minimum levels of the calculated state of charge, with $SOC_{\min}$ and $SOC_{\max}$ being the minimum and maximum limits of the storage system, respectively. These limits are imposed to increase the lifetime of the storage.

The operational algorithm, responsible for ensuring instant power balance, interacts with the load shedding/restoration optimization algorithm, the PV control, and with all of the physical components through the pulse width modulation (PWM) power converter's switching functions noted as f_A,f_B,f_C,f_{PV},f_L,f_S. The switching functions f_A,f_B,f_C are related to the three-phase converter at the PCC and are responsible for exchanging power with the main grid. The switching function f_{PV} is sent to the converter responsible for the PV system control. The switching function f_S is related with the converter used for the storage system, and the switching function f_L is a signal with information to be sent to all connected appliances, controlled individually. The load shedding/restoration optimization block receives information about the total load demand p_{L_D} and the maximum available power, being the sum of p_{PV},p_{S_D},p_{S_C} and p_{G_S} from the operational algorithm.

The load shedding/restoration block calculates then the optimum load shedding p_{L_S} to be sent back to the operational algorithm and to the load control system. The PV control block regulates the PV power to track the maximum power point or the limited power defined by the system given its necessity. The measurement block transmits information about the actual state of the system to the operational algorithm.

2.2. Operational Algorithm

As presented in [14,15], to ensure the robustness of the microgrid system it was necessary to separate the real-time control layer from the other layers (e.g., optimization layer). The operational algorithm proposed on this work was based on [6,14,15] and notoriously improved with the capability of dealing, in real-time, with the load shedding/restoration optimization algorithm which consider a real load profile and realistic constraints. The proposed operational algorithm is based on the energy management flowchart presented in [6] and aims to control and ensure power balance in real-time while respecting the storage priority strategy, as well as the imposed system's limits, as presented in Figure 4.

At the beginning of each algorithm's iteration the fixed parameters and the newest values of p_{PV}, p_L, and *soc* are set and the reference power, p^*, is then calculated as presented in Equation (1):

$$p^* = p_{PV} - p_L - C_P(v^* - v) \tag{1}$$

with C_P being the proportional gain of the controller responsible for the bus voltage stabilization, v^* the DC bus voltage reference, and v the real DC bus voltage. This power reference represents the amount of power to be supplied/absorbed to ensure the power balance of the system, and since storage and the main grid can be used to attend this necessity, a storage priority approach was proposed to define this trade-off.

Based on the resulting power reference, the usage of the grid and storage are imposed ensuring power balance while considering the proposed strategy. Based on p^*, the p_G, p_S, and PV power shed p_{PV_S} and load power shed p_{L_S}, are calculated and the real-time PWM control signals, f_A,f_B,f_C,f_{PV},f_L,f_S are sent to all dedicated converters.

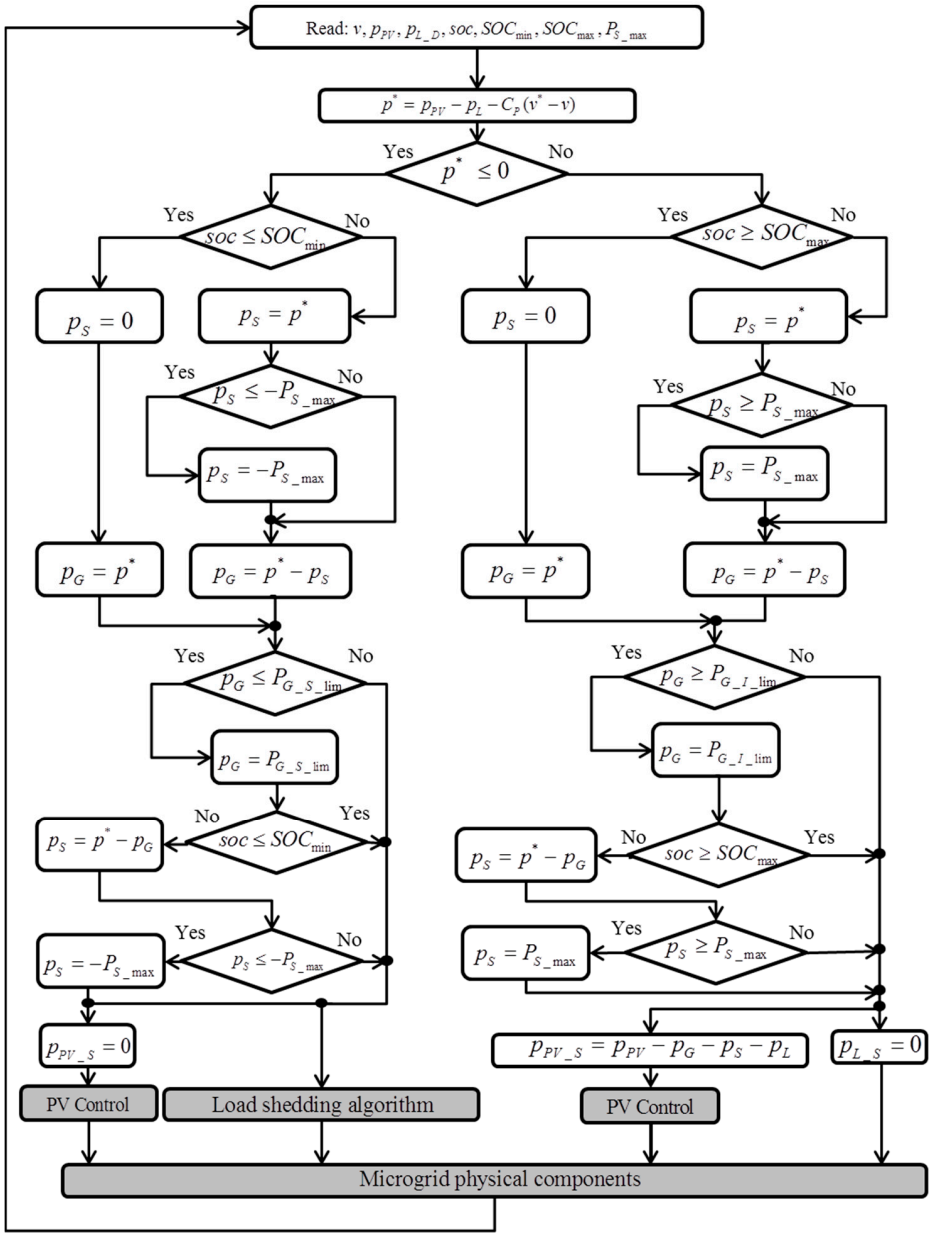

Figure 4. Operational algorithm considering the storage priority strategy.

3. Load Shedding/Restoration Optimization Algorithm

In the case where the PV production is too low or nonexistent, and the maximum allowed power to be exchanged with the storage and the main grid is already reached, but still the system would not be able to stabilize the DC bus voltage, load shedding occurs following a predefined strategy.

On the other hand, to supply the critical load limit is a necessity for commercial and industrial environments. To ensure keeping critical equipment and services operating under any circumstances, i.e., respecting the critical level imposed by the end-user, it is necessary to consider the limit imposed to the power exchanged with the main grid at least equal to the power required to supply the critical loads of the system. Otherwise, the microgrid system has to include a traditional energy source, like a micro-turbine or a diesel generator, which is necessary to start up in critical operating conditions. The proposed scenario considers a correctly-sized main grid power supply limit able to always ensure the critical load level and to perform demand-side management, based on the optimized load shedding and restoration approach.

When the microgrid is operating in limited mode, meaning that the available power from all sources is not enough to attend the load power demand, the load shedding must be used to keep the power balance and voltage stabilization. In this work the proposed load shedding method aims to be more realistic by considering each appliance with a discrete value and using an approach based on the knapsack problem to formulate the load shedding optimization problem. The proposed approach is described in detail in [17], where the main problem to be solved is to know what appliance can operate and what appliance needs to be turned off, considering a group of constraints related with the maximum time that each appliance can be shed, as well as the priority of each appliance. In this paper, the proposed load shedding/restoration approach is proposed to a DC microgrid system but this concept can be extrapolated to any microgrid architecture one could desire.

3.1. Knapsack Problem

The knapsack problem relative to load shedding/restoration cases is formulated following [18] and strongly improved concerning the appliances' restoration conditions. It can be expressed as described in Equation (2):

$$\max f(x) = \sum_{i=1}^{n} CoP_i \cdot x_i : \begin{cases} x_i = \begin{cases} 0 \text{ if } i^{th} \text{ appliance is off} \\ 1 \text{ if } i^{th} \text{ appliance is on} \end{cases} \\ 1 \leq i \leq n \end{cases}$$
$$\text{with respect to : } \begin{cases} p_L = \sum_{i=1}^{n} \mathrm{W}_i \cdot x_i \leq (p_{PV} + p_{S\_D} + p_{G\_S}) \\ CoP_i = \begin{cases} 50 \cdot CoP_{orig} \text{ if } \mathrm{t}_{count\_off} \geq T_{\max} \\ CoP_{orig} \text{ if } \mathrm{t}_{count\_on} \geq T_{\max} \end{cases} \\ \mathrm{t}_{count\_off} \geq T_{\min} \end{cases} \quad (2)$$

with $f(x)$ being the objective function, CoP_i is the coefficient of priority of i^{th} appliance, i is the appliance identification number, x_i is the decision variable of the load shedding algorithm optimization, W_i is the instant power of i^{th} appliance, CoP_{orig} is the coefficient of original priority of the i^{th} appliance, t_{count_off} is the time duration for which the appliance is shed, t_{count_on} is the time duration for which the appliance is in on-state mode, $T_{\max}$ is the maximum time duration for which the appliance can be shed, and $T_{\min}$ is the minimum time duration for which the appliance can be shed.

The definition of minimum and maximum values to the timers tied with the restoration aspect of the load control is fundamental to implement a realistic load shedding/restoration process. On one hand, these timers are vital to ensuring the smart use of the load shedding algorithm, allowing the system to reduce the impact of continuous shedding of a single appliance to the end user. On the another hand, these timers also provide a certain level of safety to the appliances, ensuring to avoid flickering a rapid and continuous connection and disconnection of energy supply, unsafe to appliances in general, but especially harmful to electronic devices. For these reasons, approaching the load shedding/restoration problem only from the point of view of the load shedding itself, without considering the restoration aspects, it is simply not enough in a realistic load shedding/restoration approach.

3.2. Load Shedding/Restoration Optimization Operation

The load shedding/restoration algorithm operates following the scheme presented in Figure 5. At the beginning, the inputs of the coefficient of priority, the minimum and maximum time, the available power, and the power demand are read and a decision is made. If the power demand is less than the power available, the algorithm does not perform the load shedding. Otherwise, when the power available is insufficient to attend the load power demand, the solver is called to perform the load shed optimization. The problem is solved by mixed integer linear programming and the CPLEX solver.

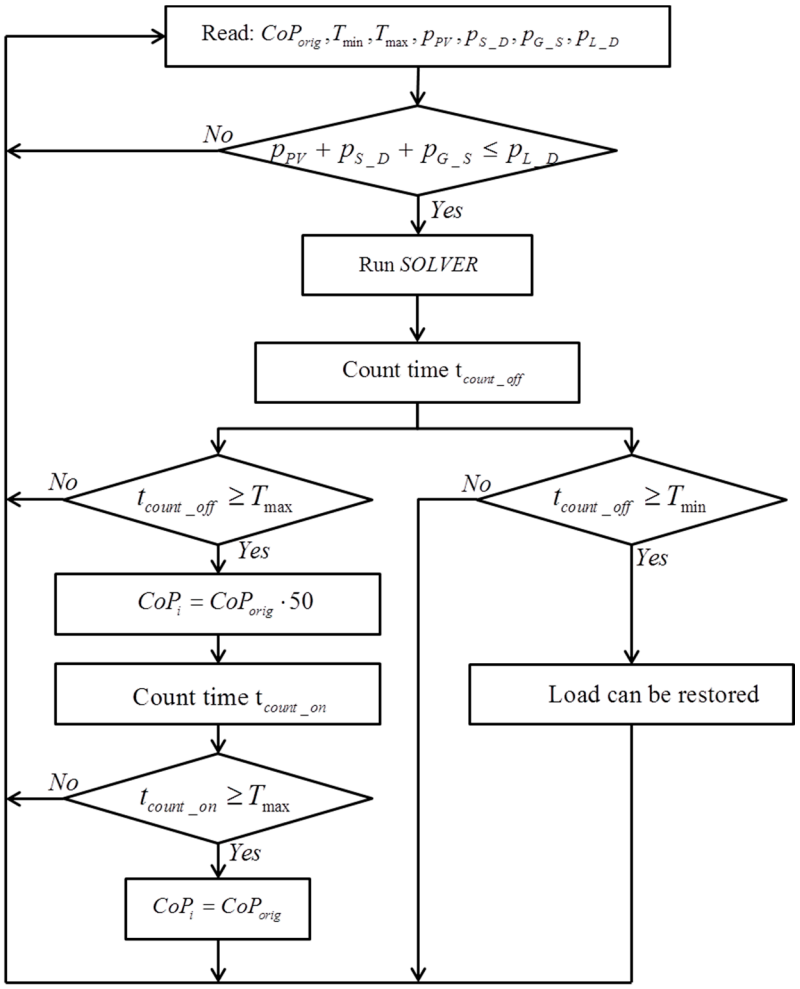

Figure 5. Load shedding/restoration optimization flow scheme.

3.3. Building Load Profile Sample

The building load profile is presented in Figure 6, with P_{L_D} being the power load demand for the given day. This profile, detailed in Table 1, is based on the historical data of the building *Pierre Guillaumat 2* from the Université de Technologie de Compiègne, France. The number of appliances and rated power were adapted to fit the physical restriction of an existing microgrid platform [2]. The designed scenario, where all appliances are fully controllable was selected to highlight the impact of considering demand-side management based on a load shedding approach in the microgrid system environment. Although a realistic scenario will have only a few controllable appliances, this will not change the concept proposed in this paper since all non-controllable loads would be considered as critical loads. This adaptation aims to allow us to validate in simulation, respecting the real dynamic of the building with the proposed load shedding approach. To perform an experimental validation it would be necessary for a load emulator to be able to control each appliance independently and, for instance, this equipment is not yet available in our microgrid platform.

The load profile considers the load power demand from 8:00–17:00, defined as a 9 h day during commercial time. After this time, from 17:00–8:00 the next morning, the main grid is assumed to supply the minimum energy consumption.

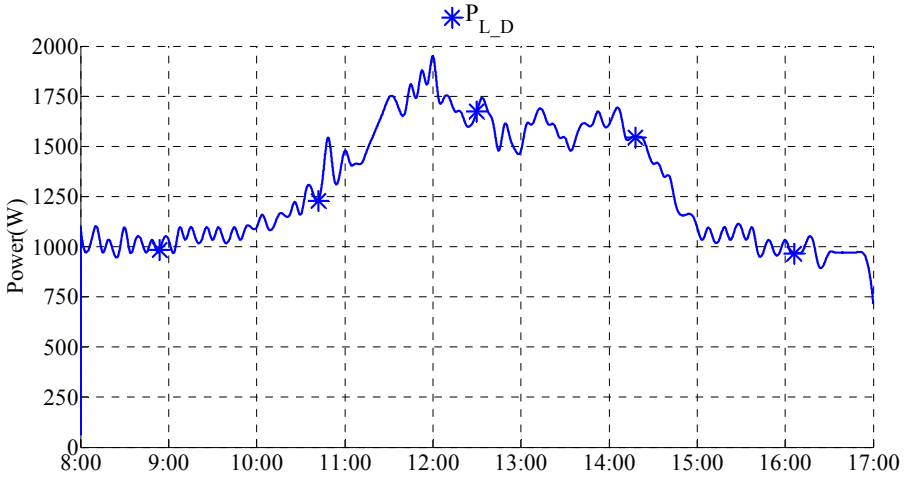

Figure 6. Building load profile sample.

Table 1. Detailed appliances profile.

i	Appliances Specifications			
	CoP_{orig}	W_{rated} (W)	T_{min} (s)	T_{max} (s)
1	5	10.8	20	100
2	100	213	120	600
3	100	7.5	20	120
4	100	25.5	120	300
5	70	52.8	20	300
6	20	250.2	30	500
7	30	21	30	500
8	1	62	20	200
9	50	33.6	20	100
10	1	131.1	30	500
11	30	30	30	180
12	2	98.4	20	600
13	20	35	20	300
14	1	208	30	500
...	...	...	...	...
49	40	37.8	20	300

It is considered that the power required to supply the maximum part of building load power is limited to 2000 W, given the physical constraints of the system. To respect this limit, the number of appliances considered to form the load profile sample presented in Figure 6 is limited to 49 different appliances, selected in such a way that the general load dynamic during the day remains the same as the real original load of the building. Table 1 shows the appliances' specifications: identification number i, coefficient of original priority CoP_{orig}, the nominal power W_{rated} of the i^{th} appliance, and time duration $T_{\min}$ and $T_{\max}$ to some of the 49 appliances.

4. Results Analysis and Discussion

The simulations are performed in the Matlab Simulink (© The MathWorks, Inc., Natick, MA, USA) environment, aiming to validate the proposed algorithmic approach and highlight the proper interaction between these algorithms while maintaining the bus voltage regulation. Section 4.1 is dedicated to detailing the microgrid behavior and voltage stability while Section 4.2 is focused on the load shedding approach.

All simulations were made considering the numerical values of parameters presented in Table 2. $k_{L_{crit}} = P_L/P_{L\_D}$ is the critical load level defined by the end-user. $P_{PV_{MPP\_STC}}$ represents the PV

generation limit, considering a PV array of 16 PV panels. C_{REF} is the storage capacity, obtained based on the available storage system described in [2]. SOC_0 is the initial state of the charge and v^* the desired voltage at the DC bus. P_{S_max} is the maximum power that can be instantly exchanged with the storage system and is set aiming to increase the storage lifetime. In this test, the chosen value is empirical, smaller than the real one. This modification is needed since the simulations are based on numerical values of the real platform; also, given the oversized storage capacity installed, if the full capacity is used, it would not be possible to see any load shedding. Therefore, P_{S_max}, SOC_{min}, SOC_{max}, $P_{G\_S\_max}$, and $P_{G\_I\_max}$ values were adapted to highlight the load shedding effect.

Table 2. System parameters.

$k_{L_{crit}}$	$P_{PV_{MPP\_STC}}$	C_{REF}	P_{S_max}	P_{L_MAX}	$P_{G\_S\_max}$	$P_{G\_I\_max}$	SOC_{min}	SOC_{max}	SOC_0	v^*
0.4	2000 W	130 Ah	800 W	2000 W	1000 W	1000 W	45%	55%	50%	400 V

4.1. Microgrid Behavior and Voltage Stability

The storage priority strategy becomes evident when analyzing the power flow P_S in Figure 7 and comparing with the state of charge behavior present in Figure 8. It is possible to see that only the storage is used until the state of charge reaches its minimum limit of 45%, presented in Table 2, as seen in Figure 8. After the minimum state of the charge limit has being reached, the system starts to exchange power with the main grid to supply the load. The storage is used again when there is a surplus of energy and it can be partially re-charged and used right after, respecting the strategy priority. A reflection of this strategy is that, since the storage is never fully charged during the day, the microgrid system does not send energy towards the main grid during a given day. The $P_{PV_{MPPT}}$ is calculated as follows:

$$P_{PV_{MPPT}} = P_{PV_{MPP\_STC}} \cdot \frac{g}{1000}[1 - \gamma(\theta - 25)] \cdot N_{PV} \quad (3)$$

with g being the solar irradiation, $P_{PV_{MPP\_STC}}$ is the PV maximum power in standard test conditions (STC), γ is the power temperature coefficient, θ is the PV cell temperature, and N_{PV} is the number of solar panels. This method is known as Osterwald's method, described in [19]. The PV cell temperature θ is estimated based on a simple and widely used approach described as follows:

$$\theta = \theta_{AIR} + g \cdot \frac{NOCT - \theta_{AIR\_TEST}}{G_{TEST}} \quad (4)$$

where the $NOCT$ is the PV cell temperature attained with free air circulation under STC and equal to 48 $^{\circ}C$, the fixed air temperature for test θ_{AIR_TEST} is equal to 20 °C, and the fixed irradiation for test G_{TEST} is defined as 800 W/m^2. The values stipulated for each variable defined before are given by the manufacturer through the datasheet of the PV panel. The usage of this specific formulation to approximate the PV cell temperature was made considering the conclusions presented in [20].

The simulation test is based on the irradiation profile from 20 May 2014 with the data measured onsite at the Université de Technologie de Compiègne—France. To better fit all of the curves in the graphic some conventions were adopted. The power exchanged with the main grid is presented as negative when the power is flowing from the main grid towards the DC microgrid system and this flow is positive when the energy in injected from the microgrid into the main grid. The storage system follows this same logic; when the storage system is supplying the load the value is negative and when the storage system is being charged the power flow is positive. Regarding the PV power curves, $P_{PV_{MPPT}}$ and P_{PV} are identical, indicating that all available PV power is consumed during the day, so that there is no PV power limitation. On the contrary, the load curves P_{L_D} and P_L are not identical and the difference between this two curves is the load shedding performed during operation. This load shedding information is identify in Figure 3 as p_{L_S}.

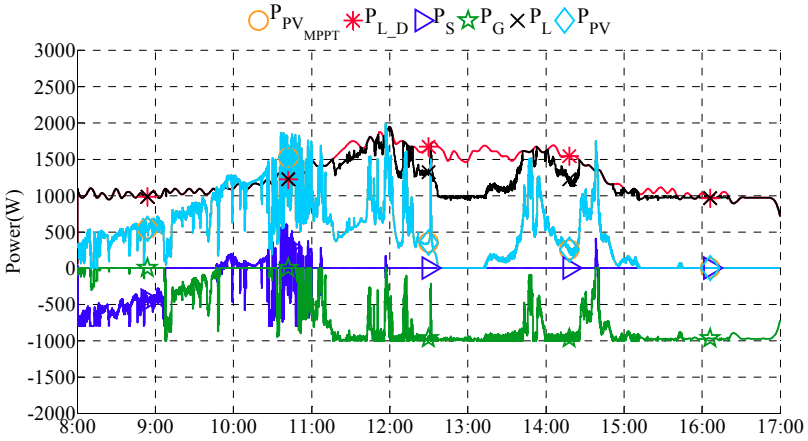

Figure 7. DC microgrid power evolution.

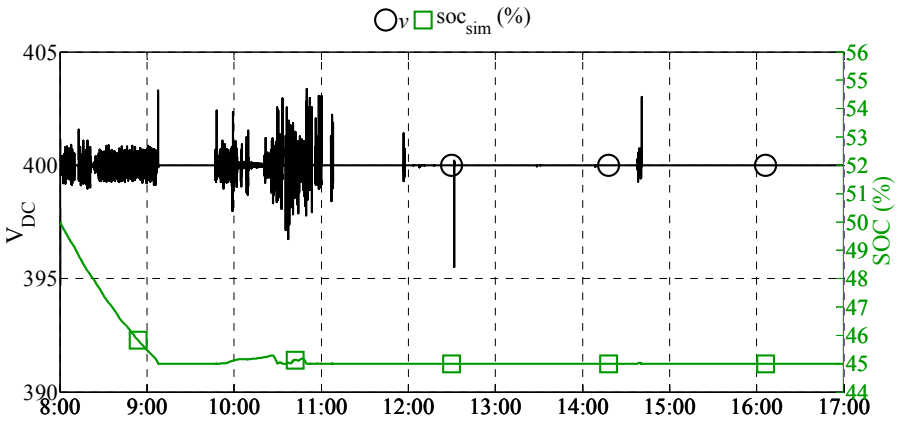

Figure 8. DC bus voltage and the state of charge evolution.

As depicted in Figures 7 and 8, the voltage stabilization is ensured while the energy management strategy is respected. The compartmentalization of the supervisory system allows more flexibility to the whole model by creating the possibility of adopting different approaches to all of the different aspects of the microgrid system, aiming to overcome specific problems, while ensuring the overall desired behavior of the system.

The critical load level phenomenon can be seen in Figure 7 between 12:30 and 13:30, where the power exchanged with the main grid reaches the imposed limit of 1000 W to ensure supply to the critical load.

Figure 8 also presents the bus voltage evolution, ν, showing that the voltage fluctuation is within acceptable limits even at the highest peak, immediately after 10:00. This fluctuation has different sources, but they are mainly caused by the control system transitory phase. The proportional control used on this simulation may not be optimally parameterized, considering that the control used was not the focus on this paper and the results presented with the given parameterization fits the idealized application. The variation seen in the bus voltage is less than 5 V, which is the equivalent of less than 1.25% of the reference value in fluctuation, an acceptable performance for the proposed system. Those results support the working assumption of the operational algorithm as a valid option to ensure voltage stabilization in the system while optimizing the load shedding.

4.2. Optimized Load Shedding Results

Regarding the load shedding aspect of the simulation, Figure 9 presents the attended load evolution, k_L defined as follow: when k_L is equal one, no load shedding is performed and the entire load power demand is attended. When the load is partially shed, for example when k_L is 0.60, it means that 40% of the load it is not supplied, therefore 40% of the load is shed. The dotted blue line marks the $k_{L_{crit}}$ which is the critical limit imposed by the end-user. This limit stipulates that 40% of the load demand shall not be shed and must be permanently supplied. The system is then able to respect the limit imposed by the end-user while keeping the voltage stabilization and performing an optimizing load shedding.

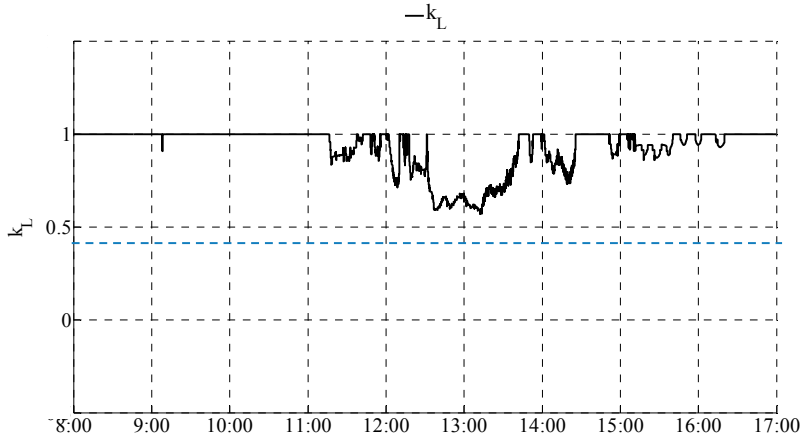

Figure 9. Load shed percentage evolution.

In Figure 9 it is possible to see that, during the day, the load shedding is performed as needed, but the critical limit of 40% is never reached. In fact, the maximum load shedding does not even arrive at 50%, meaning that the proposed scenario was well designed considering the necessity of constant supply of the critical loads, while respecting the grid power exchange limit.

Figure 10 presents a zoomed area from the power flow presented in Figure 7. The first remarkable characteristic about this figure is the simulated load power, the dark line. This pattern is a reflex of each appliance having a realistic discrete value considered during the load shedding optimization. In addition to the load power, it is possible to see that the power exchanged with the main grid, the green line, it is not near its limit all of the time. This is counterintuitive since we aim to use all available power to minimize load shedding but, in fact, since the appliances have a realistic discrete dynamic, the fluctuation in the grid power flow actually indicates that this small amount of energy that is not being used it is not enough to attend the rated power of any appliance that has been shed. Therefore, to keep the system's power balance, the power available from the main grid is not exactly fully exploited.

One example of the flexibility of this approach is that even if the load power optimization has a computational cost, it takes a fraction of the time (about 0.5 s) more while performing the optimization shown in Figure 10, rather than being non-optimized at all. The voltage stabilization is ensured by the control system allowing the solution to be applied without sacrificing the robustness of the system.

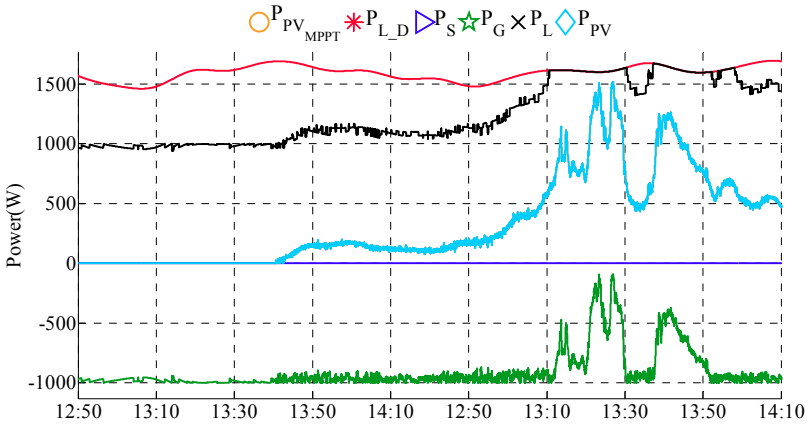

Figure 10. Load shed detail.

5. Conclusions

First and foremost, the microgrid system is an answer to the necessity of increasing the renewable energy penetration in a sustainable way to maximize the use of renewable energies, and reducing the consumption of fossil fuels and other non-renewable sources. When it comes to commercial building applications, some of the challenges were addressed in this paper, such as ensuring voltage stabilization and increasing reliability by actively ensuring power balance. Compared with the literature and previous works, the improvement comes from a demand-side management strategy. This strategy was proposed based on a critical load limit and on a load shedding/restoration optimization algorithm ensured during operation. In addition, the proposed strategy was validated through simulation tests and is based on a realistic load curve, which was built based on real building consumption. Furthermore, the supervisory controller can be further elaborated either by programming a digital signal processor (DSP) with the C programming language, or by programming a controller based on field programmable gate arrays (FPGA) (e.g., Xilinx ISE), so that it can have applications in the industrial field. In the environments where DC loads are becoming predominant, the usage of a DC microgrid architecture can improve the overall efficiency of the system, avoiding a waste of energy in the consecutive transformation from DC to AC and back to DC, before finally being consumed by the load. The whole microgrid architecture described on this paper was designed to create a flexible system. This approach, when applied in a commercial building or industry, allows the user to have the best trade-off between reducing the energy cost, ensuring voltage stabilization, increasing robustness, and maximizing renewable energy penetration, while respecting the main grid limitations and allowing the system operator to act more efficiently without stopping any critical operations on site. This flexible system goal is achieved by the integration of different algorithms interacting based on a management system that handles the dichotomy between the different approaches and the instant power balance. In future works, to obtain the most of this flexibility, different approaches for the management strategy shall be implemented, based on optimization methods, aiming to decrease the energy cost to the end user.

Author Contributions: All authors have conceived and designed the system, performed the experiments, and analyzed the data. All authors contributed jointly to the writing and preparing revision of this manuscript. All authors have read and approved the manuscript.

Conflicts of Interest: The authors declare no conflict of interest and the founding sponsors had no role in the design of the study; in the collection, analyses, or interpretation of data; in the writing of the manuscript, and in the decision to publish the results.

References

1. Patterson, B. DC, Come Home: DC Microgrids and the Birth of the "Enernet". *IEEE Power Energy Mag.* **2012**, *10*, 60–69. [CrossRef]
2. Wang, B.; Sechilariu, M.; Locment, F. Intelligent DC Microgrid with Smart Grid Communications: Control Strategy Consideration and Design. *IEEE Trans. Smart Grid* **2012**, *3*, 2148–2156. [CrossRef]
3. Guerrero, J.; Chandorkar, M.; Lee, T.; Loh, P. Advanced Control Architectures for Intelligent Microgrids Part I: Decentralized and Hierarchical Control. *IEEE Trans. Ind. Electron.* **2013**, *60*, 1254–1262. [CrossRef]
4. Justo, J.J.; Mwasilu, F.; Lee, J.; Jung, J.W. AC-microgrids versus DC-microgrids with distributed energy resources: A review. *Renew. Sustain. Energy Rev.* **2013**, *24*, 387–405. [CrossRef]
5. Dragicevic, T.; Guerrero, J.; Vasquez, J.; Skrlec, D. Supervisory Control of an Adaptive-Droop Regulated DC Microgrid with Battery Management Capability. *IEEE Trans. Power Electron.* **2014**, *29*, 695–706. [CrossRef]
6. Sechilariu, M.; Wang, B.; Locment, F. Building Integrated Photovoltaic System with Energy Storage and Smart Grid Communication. *IEEE Trans. Ind. Electron.* **2013**, *60*, 1607–1618. [CrossRef]
7. Sabzehgar, R. A review of AC/DC microgrid-developments, technologies, and challenges. In Proceedings of the 2015 IEEE Green Energy and Systems Conference (IGESC), Long Beach, CA, USA, 9 November 2015; pp. 11–17.
8. Kumar, Y.V.P.; Bhimasingu, R. Review and retrofitted architectures to form reliable smart microgrid networks for urban buildings. *IET Netw.* **2015**, *4*, 338–349. [CrossRef]
9. Faranda, R.; Pievatolo, A.; Tironi, E. Load Shedding: A New Proposal. *IEEE Trans. Power Syst.* **2007**, *22*, 2086–2093. [CrossRef]
10. Mokhlis, H.; Karimi, M.; Shahriari, A.; Abu Bakar, A.; Laghari, J. A new under-frequency load shedding scheme for islanded distribution network. In Proceedings of the 2013 IEEE PES Innovative Smart Grid Technologies (ISGT), Washington, DC, USA, 24–27 February 2013; pp. 1–6.
11. Shokooh, F.; Dai, J.; Shokooh, S.; Taster, J.; Castro, H.; Khandelwal, T.; Donner, G. An intelligent load shedding (ILS) system application in a large industrial facility. In Proceedings of the Conference Record of the 2005 IEEE Industry Applications Conference fortieth IAS Annual Meeting, Hong Kong, China, 2–6 October 2005; Volume 1, pp. 417–425.
12. Xu, L.; Chen, D. Control and Operation of a DC Microgrid with Variable Generation and Energy Storage. *IEEE Trans. Power Deliv.* **2011**, *26*, 2513–2522. [CrossRef]
13. Balog, R.S.; Weaver, W.W.; Krein, P.T. The Load as an Energy Asset in a Distributed DC SmartGrid Architecture. *IEEE Trans. Smart Grid* **2012**, *3*, 253–260. [CrossRef]
14. Sechilariu, M.; Wang, B.C.; Locment, F. Supervision control for optimal energy cost management in DC microgrid: Design and simulation. *Int. J. Electr. Power Energy Syst.* **2014**, *58*, 140–149. [CrossRef]
15. Sechilariu, M.; Wang, B.C.; Locment, F.; Jouglet, A. DC microgrid power flow optimization by multi-layer supervision control. Design and experimental validation. *Energy Convers. Manag.* **2014**, *82*, 1–10. [CrossRef]
16. Sechilariu, M.; Locment, F.; Wang, B. Photovoltaic Electricity for Sustainable Building. Efficiency and Energy Cost Reduction for Isolated DC Microgrid. *Energies* **2015**, *8*, 7945–7967. [CrossRef]
17. Khoa, T.D.; Dos Santos, L.T.; Sechilariu, M.; Locment, F. Load Shedding and Restoration Real-Time Optimization for DC Microgrid Power Balancing. In Proceedings of the 2016 IEEE International Energy Conference (ENERGYCON), Leuven, Belgium, 4–8 April 2016.
18. Lamedica, R.; Santini, E.; Teodori, S.; Romito, D.Z. Electrical loads management in energy emergency conditions. *Int. J. Electr. Power Energy Syst.* **2015**, *66*, 86–96. [CrossRef]
19. Osterwald, C. Translation of device performance measurements to reference conditions. *Sol. Cells* **1986**, *18*, 269–279. [CrossRef]
20. Denoix, T.; Sechilariu, M.; Locment, F. Experimental comparison of photovoltaic panel operating cell temperature models. In Proceedings of the IECON 2014—40th Annual Conference of the IEEE Industrial Electronics Society, Dallas, TX, USA, 29 October–1 November 2014; pp. 2089–2095.